



**Fermi National Accelerator Laboratory**

**FERMILAB-Conf-98/002**

## **Production and Fragmentation of Heavy Quarks**

Austin Napier

E791 Collaboration

*Fermi National Accelerator Laboratory  
P.O. Box 500, Batavia, Illinois 60510*

*Tufts University  
Medford, MA 02155*

January 1998

Published Proceedings of the *XVII International Conference on Physics in Collision*,  
University of Bristol, Bristol, UK, June 25-27, 1997

## **Disclaimer**

*This report was prepared as an account of work sponsored by an agency of the United States Government. Neither the United States Government nor any agency thereof, nor any of their employees, makes any warranty, expressed or implied, or assumes any legal liability or responsibility for the accuracy, completeness, or usefulness of any information, apparatus, product, or process disclosed, or represents that its use would not infringe privately owned rights. Reference herein to any specific commercial product, process, or service by trade name, trademark, manufacturer, or otherwise, does not necessarily constitute or imply its endorsement, recommendation, or favoring by the United States Government or any agency thereof. The views and opinions of authors expressed herein do not necessarily state or reflect those of the United States Government or any agency thereof.*

## **Distribution**

*Approved for public release; further dissemination unlimited.*

# Production and Fragmentation of Heavy Quarks <sup>a</sup>

Austin Napier  
*High Energy Physics, Tufts University, Medford,  
MA 02155, USA*

This talk is a review of recent results on the production and fragmentation of heavy quarks from fixed target experiments, from  $e^+e^-$  and  $p\bar{p}$  colliders, and from HERA.

## 1 Introduction

This review is primarily devoted to charm and bottom quarks; only the top quark cross section measurement is discussed. An excellent and extensive review on the production of heavy quarks appeared a few months ago by Frixione et al.<sup>1</sup> We will refer to this review by the authors' initials (FMNR).

## 2 Forward Cross Sections from Fixed Target Experiments

Figure 1 shows cross sections from fixed-target experiments as presented in FMNR<sup>1</sup> for  $c\bar{c}$  and  $b\bar{b}$  production from  $\pi^-$ -N collisions as a function of beam energy. The solid curves give the predictions of next-to-leading order (NLO) QCD calculations<sup>1</sup>, using c and b quark masses of  $m_c = 1.5$  GeV and  $m_b = 4.75$  GeV. The lower curve has the scale parameter set to  $\mu_0/2$  and the upper curve is for  $2\mu_0$  where the default scale parameters ( $\mu_0$ ) are taken as  $\mu_R = m_c$  (renormalization scale) and  $\mu_F = 2m_c$  (factorization scale) for charm and  $\mu_R = m_b$  and  $\mu_F = m_b$  for bottom. This band provides an estimate of the theoretical uncertainty in the predictions. Also shown are the predictions obtained by varying the heavy quark masses, with the dotted curves corresponding to  $m_c = 1.8$  GeV and  $m_b = 5$  GeV and the dashed curves corresponding to  $m_c = 1.2$  GeV and  $m_b = 4.5$  GeV. Larger values of the heavy quark mass correspond to smaller cross sections. Given the large errors on the b-quark cross sections, the data appear to be well-described by the predictions. It should be noted that Fermilab E706 has added a new point to the charm data at 515 GeV since the FMNR review. E706 reports a forward cross section for  $D^\pm$  production of  $11.4 \pm 2.7 \pm 3.3 \mu\text{b}^2$ . Figure 2 shows the cross sections from fixed-target experiments<sup>1</sup> for production of c and b quarks from p-N interactions. Theoretical predictions are again shown as a band limited by two values

---

<sup>a</sup>Invited talk presented at the XVII International Conference on Physics In Collision, University of Bristol, Bristol, U.K., June 25, 1997.

of the scale parameters, and using the 3 values (each) for the c and b quark masses. If the two figures are overlaid, we note that the data points for both pion and proton beams are consistent with each other. More data on b-quark production near threshold is needed to verify that the proton cross section is significantly smaller than the pion predictions. J. Smith and R. Vogt<sup>3</sup> have calculated c and b quark cross sections near threshold, including an “all order resummation of initial state soft-plus-virtual gluon radiation.”

New cross section results for inclusive production of  $D^0$  and  $\bar{D}^0$ ,  $D^\pm$ , and  $D_s^\pm$  are available from the CERN WA92 collaboration<sup>4</sup>, and these results are shown in Figure 3, together with results from other experiments. All results are for  $\pi^-$  beam on nuclear targets.

### 3 Differential Cross Sections

Differential cross sections in Feynman-x ( $x_F$ ) and transverse momentum squared ( $p_t^2$ ) of D and B mesons are often used to aid understanding of the production mechanisms of c and b quarks. Figure 4 shows the Feynman-x distribution for D mesons from Fermilab E769<sup>5</sup> for three different incident beams at 250 GeV. We note that FMNR<sup>1</sup> predict the proton beam will produce fewer charm mesons than the pion beam for Feynman-x values larger than 0.2, in agreement with data. Figure 5 shows the  $p_t^2$  distribution from E769. In this case, the proton and pion beam data are consistent with each other. The statistical significance of the data at high  $p_t^2$  is not sufficient to discriminate between the pion and proton predictions, although the proton data are consistent with theory.

It should be noted that the theoretical predictions in Figures 4 and 5 were made using bare charm quarks; no fragmentation was included. If the Peterson et al.<sup>6</sup> fragmentation function is included, the theory predicts curves which are too “soft” to match the data. However, it has been observed<sup>1</sup> that if 1 GeV intrinsic transverse momentum of the incoming partons is included, the theory curves can be brought into agreement with the data. FMNR choose an intrinsic  $k_t^2$  for each incoming parton (i.e. gluon) at random from a gaussian distribution, and include fragmentation effects by convoluting the cross section with a fragmentation function<sup>6</sup>. The most accurate determinations of fragmentation functions are taken from LEP-1 data. For example, Figure 6 shows the ALEPH<sup>7</sup> data from 1.46 million  $Z^0$  decays to b-quarks, with three different parameterizations of the heavy quark fragmentation function. Recently, Fermilab E706<sup>2</sup> has examined  $D^\pm$  production from a  $\pi^-$  beam at 515 GeV for  $p_t$  up to 7 GeV, significantly higher than the data from E769 and WA92. If fragmentation is included, the best agreement is obtained if an intrinsic  $k_t^2$

between 1 and 2 GeV<sup>2</sup> is used. The bare charm NLO prediction appears to fall too slowly to match the data, particularly at high  $p_t$ , as shown in figure 7.

#### 4 Heavy Quark Pairs

Events in which both the heavy quark and antiquark decays are reconstructed provide a more sensitive test of QCD predictions. Several experiments including WA75, WA92, and Fermilab E791 (see FMNR for references) have reported distributions of the azimuthal angle between two charm mesons. Figure 8 shows WA92 data<sup>8</sup> for  $\pi N$  collisions. The NLO QCD prediction is strongly peaked at 180°. Adding an intrinsic  $k_t$  reduces this effect. Adding fragmentation has no effect on these distributions, since the fragmentation function only affects the momentum and not the particle direction. An intrinsic  $k_t^2$  value of 1 GeV<sup>2</sup> seems in good agreement with the data. FMNR<sup>1</sup> observe that photoproduction data (NA10 and Fermilab E691 and E687) are also consistent with non-zero  $k_t^2$ , however, the optimum value may be more like 0.5 GeV<sup>2</sup>, lower than observed in hadron beams. D0 has measured the azimuthal angle ( $\Delta\Phi$ ) between b-quark jets. Figure 9 shows the angle between muons from b-quarks from D0 compared with the HVQJET program<sup>9</sup>. The shape of the distribution is well fit. Contributions from leading order flavor creation, and NLO diagrams for flavor excitation, gluon splitting, and gluon radiation have been included.

#### 5 Fragmentation Functions

Fragmentation functions are not calculated entirely from first principles, and experimental input is required. The Peterson parameterization<sup>6</sup> has long been used successfully for charm mesons. Recently Binnewies, Kniehl, and Kramer<sup>10</sup> have obtained new sets of fragmentation functions for  $D^{*\pm}$  mesons by fitting LEP-1 data, and find that they agree nicely with HERA data (see section 8).

There is still relatively little data on charm and beauty baryon production, however, there are new calculations of these fragmentation functions, based on a diquark model<sup>11</sup>. In this model, an off-shell heavy quark radiates a gluon which produces a diquark-antidiquark ( $\overline{D}\overline{D}$ ) pair. This is calculated in perturbative QCD with form factors for  $g \rightarrow \overline{D}\overline{D}$  near threshold for on-shell diquarks. The heavy quark plus the diquark then produce a charm baryon. This is calculated using a non-relativistic confining potential model consistent with the baryon spectrum. The anomalous chromomagnetic moment is a free parameter, chosen to agree with the light baryon spectrum. One can then integrate over the heavy quark virtuality (or  $p_T(\overline{D})$ ) and over all  $\overline{D}$  to get the fragmentation functions  $D_Q^{B\varphi}(z, \mu_0^2)$ . QCD evolution via Altarelli-Parisi then

gives  $D_Q^{B_Q}(z, Q^2)$ . These functions were used to calculate the probability for production of a baryon  $B_Q$  containing a heavy quark  $Q$ . The spin dependent forms can be used to get the baryon polarization. Figure 10 shows the spin-averaged fragmentation functions for the  $\Xi_c$  states at  $Q = \mu_0$  and at 5.5 GeV. In Figure 10c the prediction for  $\Xi_c^*(3/2)$  can be compared with data from CLEO<sup>12</sup>. Note that the baryon fragmentation functions predict a peak near 0.83-0.84 unlike the Peterson form<sup>6</sup> used for mesons. The data show no indication of this peak, however statistics are quite low for the only data point in the region above 0.8 in  $z$  (at 0.9). Adamov and Goldstein<sup>11</sup> also calculate the fragmentation probabilities (found by integrating from  $z = 0$  to  $z = 1$ ) for producing various charm and bottom baryons. These predictions agree quite well with LEP-1 and CLEO data for  $\Lambda_c$ ,  $\Lambda_b$ ,  $\Sigma_b$ , and  $\Xi_c^*$ .

## 6 Leading Particle Effects

Leading particle effects have been observed for charm (D) production from pion beams in CERN WA82<sup>13</sup>, Fermilab E769<sup>14</sup> and E791<sup>15</sup>, and recently by CERN WA92<sup>4</sup>. The asymmetry parameter can be defined as  $A = (\sigma_L - \sigma_{NL}) / (\sigma_L + \sigma_{NL})$  where L refers to a “leading” charm meson (containing a valence quark or antiquark from the incident beam) and NL refers to a “non-leading” charm meson (which does not contain such a valence quark or antiquark). Figure 11 shows the WA92 data<sup>4</sup> as a function of Feynman- $x$  and  $p_t^2$ , compared to predictions of the LUND model. Note the rise in asymmetry as  $x$  increases from zero to one. The lower half of the figure shows the asymmetry as a function of  $p_t^2$ . In this variable the distributions are consistent with a constant value. E791 has searched for asymmetry in  $D_s$  production<sup>16</sup>. Figure 12 shows the data compared to  $D^\pm$  data from the same experiment. For  $D_s$ , there are no leading particles, so no asymmetry is expected, and the results are consistent with none. E791 also has a large sample of  $\Lambda_c$ ’s and results are expected soon. E791<sup>15</sup> found that the LUND program PYTHIA can be “tuned” to produce good agreement with the observed  $D^\pm$  asymmetries. This is done by adjusting the parameters for the charm quark mass, the average  $k_t^2$ , and the diquark splitting fraction.

## 7 A-dependence

The atomic number dependence of inclusive cross sections for D mesons has been of interest for many years. Most fixed target experiments have measured forward cross sections consistent with the form  $\sigma = \sigma_0 A^\alpha$  with  $\alpha$  near one, as expected from QCD arguments. Two experiments with good statistics are

CERN WA82<sup>17</sup> and Fermilab E769<sup>18</sup>. CERN WA92<sup>4</sup> has now reported values for both charged and neutral D mesons. They find  $\alpha = 0.92 \pm 0.07 \pm 0.02$  for  $D^0, \overline{D}^0$ ,  $\alpha = 0.95 \pm 0.07 \pm 0.03$  for  $D^+, D^-$ , and  $\alpha = 1.12 \pm 0.30 \pm 0.03$  for  $D_s^+, D_s^-$ . These values are consistent with E769<sup>18</sup> and WA82<sup>17</sup> measurements, but not with beam dump measurements which gave considerably lower values<sup>19</sup>. A possible explanation for this effect is that the beam dump experiments may be more sensitive to large Feynman-x values where the value of  $\alpha$  may be smaller. Unfortunately, at present there are insufficient data from fixed target experiments to study the variation of  $\alpha$  with Feynman-x. Earlier experiments which studied the production of strange particles found that  $\alpha$  decreases with increasing Feynman-x<sup>20</sup>. Fermilab E772 charmonium results show this behavior, and it is also expected for charm mesons.

## 8 Results from HERA

The virtual photons from positron-proton collisions at HERA provide an opportunity to study photoproduction above 100 GeV in the  $\gamma p$  center of mass. Figure 13 (from FMNR<sup>1</sup>) shows  $c\bar{c}$  data from ZEUS and H1 as well as lower energy data from CERN NA14, Fermilab E687 and E691. A clean  $D^{*\pm}$  signal has been observed by ZEUS<sup>21</sup>, using the  $D \rightarrow K\pi$  decay, and the differential cross sections ( $d\sigma/dp_t$  where  $p_t$  is the transverse momentum of the  $D^*$ ) have been compared with NLO QCD using a massive charm approach<sup>22</sup> and a massless charm approach<sup>23</sup>. The latter gives better agreement with data. In the massless approach, charm is considered to be one of the active flavors (along with u,d,s) and  $m_c$  is neglected for  $p_T \gg m_c$ . Differential distributions with respect to W ( $\gamma p$  center of mass energy, range 115-280 GeV) and  $\eta$  (pseudorapidity, range -1.5 to 1.0) also show better agreement with the massless charm approach. However, the errors on the data points are large, and the massive charm approach is not ruled out.

## 9 B-physics at the Fermilab Tevatron

Inclusive b-quark cross sections are now well-measured by CDF and D0. Figure 14a shows the D0 results<sup>9</sup> for the inclusive cross section  $\sigma^b(p_t^b > p_t^{min})$  measured using dimuons, inclusive single muons, and from  $J/\Psi$  production. NLO QCD predictions<sup>1</sup> agree with the shape of the spectrum, but underestimate the magnitude of the cross section by a factor of 2. CDF<sup>24</sup> has reported a slightly larger factor of 2.5. D0 has measured the forward cross section for muons from b decay. Figure 14b shows the differential distribution

$d^2\sigma_b^\mu/dp_t^\mu dy^\mu$ , for  $2.4 < y < 3.2$ . Here the data are a factor of 4 higher than the NLO QCD prediction.

Recently, CDF and D0 obtained data at lower energy (630 GeV) which allowed direct comparison with UA1 data. Figure 14c shows this comparison<sup>9</sup>. Again, the data are about a factor of two higher than the NLO QCD predictions. Taking the ratio of 630 GeV data to 1800 GeV data cancels many uncertainties, both experimental and theoretical, and NLO QCD predictions are in good agreement as shown in Figure 14d. Figure 15a shows  $d\sigma_b^\mu/dy^\mu$  for  $p_t^\mu > 5$  GeV/c and for  $p_t^\mu > 8$  GeV/c respectively. The disagreement with theory appears to increase as rapidity increases.

Both CDF and D0 have substantial  $J/\Psi$  signals. CDF has studied prompt production of  $J/\Psi$ <sup>27</sup> for  $\eta < 0.6$  and found that most of the production is direct ( $64 \pm 6\%$ ) as opposed to originating from the decay of  $\chi_c$  and  $\Psi(2S)$ . Figure 15b shows the  $(d\sigma/dp_t) \times BR$  distribution. Recently D0 studied forward production in the range  $2.5 < \eta^{J/\Psi} < 3.7$ . Figure 15c shows the  $p_T$  dependence of the  $J/\Psi$  data<sup>9</sup>. A significant part of the signal comes from b decays, and the fraction increases with  $p_T$ . Prompt color singlet c decays<sup>25</sup> fail to describe the data. A model with color octet contributions<sup>26</sup>, using parameters obtained by fits to central rapidity prompt  $J/\Psi$  production, agrees reasonably well with the forward data.

CDF has observed prominent  $\Upsilon$  signals<sup>29</sup>. Clear separation of the  $\Upsilon$ ,  $\Upsilon'$ , and  $\Upsilon''$  is seen.  $d\sigma/dp_t dy$  times BR for  $\Upsilon(1S)$  and  $\Upsilon(2S)$  have been compared with QCD calculations<sup>30</sup>. The data diverge from predictions as  $p_t$  increases. LEP experiments have not seen excess  $\Upsilon$  production. L3 searched for both  $\mu^+\mu^-$  and  $e^+e^-$  decays in the LEP-1 data. One candidate falls in the expected mass range, and they can only set upper limits on  $\Upsilon$  production<sup>31</sup>. These results, and those from HERA, seem to provide no support for color octet models.

## 10 Top Quark Production

Top quark physics will be discussed by another speaker, so here we consider only the cross section measurement. The CDF and D0 results have recently been presented by Paulini<sup>30</sup>. Both CDF and D0 results lie above the QCD predictions of 4.55 to 5.50 pb. CDF finds  $\sigma_{t\bar{t}} = 7.5 + 1.9 - 1.6$  pb and D0 finds  $\sigma_{t\bar{t}} = 5.77 \pm 1.76$  pb. The cross section for  $t\bar{t}$  production depends on the mass of the top quark as shown in Figure 15d<sup>9</sup>.

## 11 Summary

NLO QCD has been quite successful in describing many features of open heavy quark production. Shapes of many differential distributions are well described. Although some absolute predictions may disagree with data by factors of 2-4 at present, these discrepancies do not seem serious.

It is encouraging to see that fragmentation functions are now consistent with fixed target charm production data, provided some intrinsic transverse momentum is given to the incident partons. The parton distribution functions and fragmentation functions are not calculated from first principles, and require input from experiments. More work is needed to explain leading particle effects seen in fixed target charm production.

The profuse  $J/\psi$  and  $\Upsilon$  production seen in  $p\bar{p}$  collisions needs explanation. No excess is observed at LEP or HERA, where the color singlet model<sup>25</sup> appears to work well. Color octet contributions<sup>26</sup> have been introduced to explain the Tevatron data, however these do not appear consistent with the HERA data.

In the near future, we look forward to b-quark physics from ZEUS and H1 after the HERA intensity upgrade, and to new c-quark results from high statistics fixed target experiments at Fermilab (FOCUS, SELEX) and at CERN (WA89). Results on b-physics continue to emerge from CLEO, CDF, and D0, and soon we will have physics from HERA-B, BaBar (SLAC), and Belle (KEK). In the future there will be experiments at the LHC and BTeV.

## Acknowledgments

It is a pleasure to thank the U.S. Department of Energy for support, the experimenters and theorists who shared their recent results, and the conference organizers for a highly successful and informative conference.

## References

1. S. Frixione, M.L. Mangano, P. Nason, and G. Ridolfi, CERN-TH/97-16, hep-ph/9702287, to appear in "Heavy Flavours II", eds. A.J. Buras and M. Lindner, World Scientific (Singapore).
2. L. Apanasevich *et al.*, *Phys. Rev. D* **56**, 1391 (1997).
3. J. Smith and R. Vogt, *Z. Phys. C* **75**, 271 (1997).
4. M.I. Adamovich *et al.*, *Nucl. Phys. B* **495**, 34 (1997).
5. G.A. Alves *et al.*, *Phys. Rev. Lett.* **77**, 2388 (1996), *Phys. Rev. Lett.* **77**, 2392 (1996).

6. C. Peterson *et al.*, *Phys. Rev. D* **27**, 105 (1983).
7. D. Buskulic *et al.*, *Phys. Lett. B* **357**, 699 (1995).
8. M.I. Adamovich *et al.*, *Phys. Lett. B* **385**, 487 (1996).
9. R. Jesik, D0 Collaboration, private communication.
10. J. Binnewies *et al.*, *Z. Phys. C* **76**, 677 (1997) .
11. A.D. Adamov and Gary R. Goldstein, *Phys. Rev. D* **56**, 7381 (1997).
12. L. Gibbons *et al.*, *Phys. Rev. Lett.* **77**, 810 (1996).
13. M. Adamovich *et al.*, *Phys. Lett. B* **305**, 402 (1993).
14. G.A. Alves *et al.*, *Phys. Rev. Lett.* **72**, 812 (1994), *Phys. Rev. Lett.* **72**, 1946 (1994).
15. E.M. Aitala *et al.*, *Phys. Lett. B* **371**, 157 (1996).
16. E.M. Aitala *et al.*, *Phys. Lett. B* **411**, 230 (1997).
17. M.I. Adamovich *et al.*, *Nucl. Phys. (Proc. Suppl.)* **B27**, 212 (1992).
18. G.A. Alves *et al.*, *Phys. Rev. Lett.* **70**, 722 (1993).
19. M.E. Duffy *et al.*, *Phys. Rev. Lett.* **55**, 1816 (1985), H.Cobbaert *et al.*, *Phys. Lett. B* **206**, 546 (1988).
20. D.S. Barton *et al.*, *Phys. Rev. D* **27**, 2580 (1983).
21. J. Breitweg *et al.*, *Phys. Lett. B* **401**, 192 (1997).
22. S. Frixione *et al.*, *Nucl. Phys. B* **454**, 3 (1995).
23. B.A. Kniehl *et al.*, *Z. Phys. C* **76**, 689 (1997).
24. F. Stichelbaut, for the CDF and D0 Collaborations, XXXII Rencontre de Moriond, *QCD and High Energy Interactions*, March 22-24, 1997, FERMILAB-97-159-E.
25. See for example, E.L. Berger and D. Jones, *Phys. Rev. D* **23**, 1521 (1981), R. Baier and R. Ruckl, *Z. Phys. C* **19**, 251 (1983).
26. E. Braaten and S. Fleming, *Phys. Rev. Lett.* **74**, 3327 (1995), M. Cacciari *et al.*, *Phys. Lett. B* **356**, 553 (1995).
27. F. Abe *et al.*, *Phys. Rev. Lett.* **79**, 572 (1997).
28. F. Abe *et al.*, *Phys. Rev. Lett.* **79**, 578 (1997).
29. F. Abe *et al.*, *Phys. Rev. Lett.* **75**, 4358 (1995).
30. M. Paulini, hep-ex/9701019, in Proc. 24th SLAC Summer Institute, Aug. 1996, FERMILAB-Conf-96-456-E.
31. M. Acciarri *et al.*, CERN-PPE-97-078, submitted to *Phys. Lett. B*.

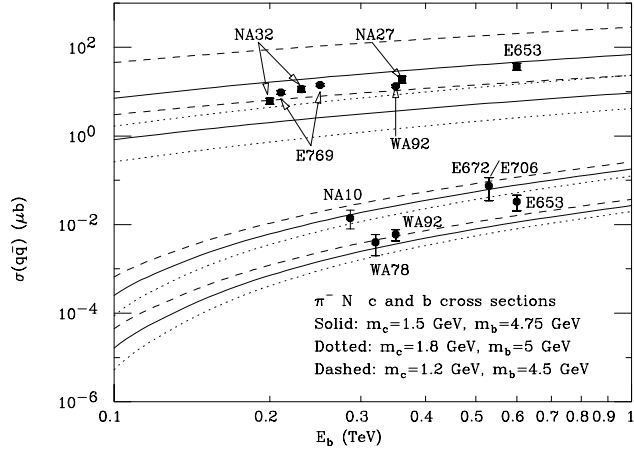


Figure 1: Cross sections for  $c\bar{c}$  and  $b\bar{b}$  from  $\pi^-$ -N collisions.

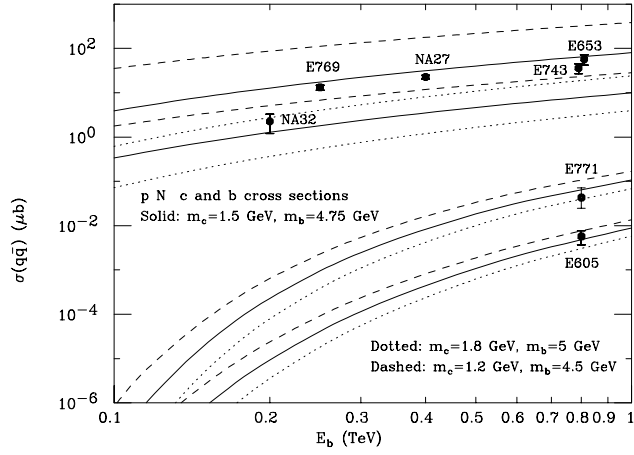


Figure 2: Cross sections for  $c\bar{c}$  and  $b\bar{b}$  from p-N collisions.

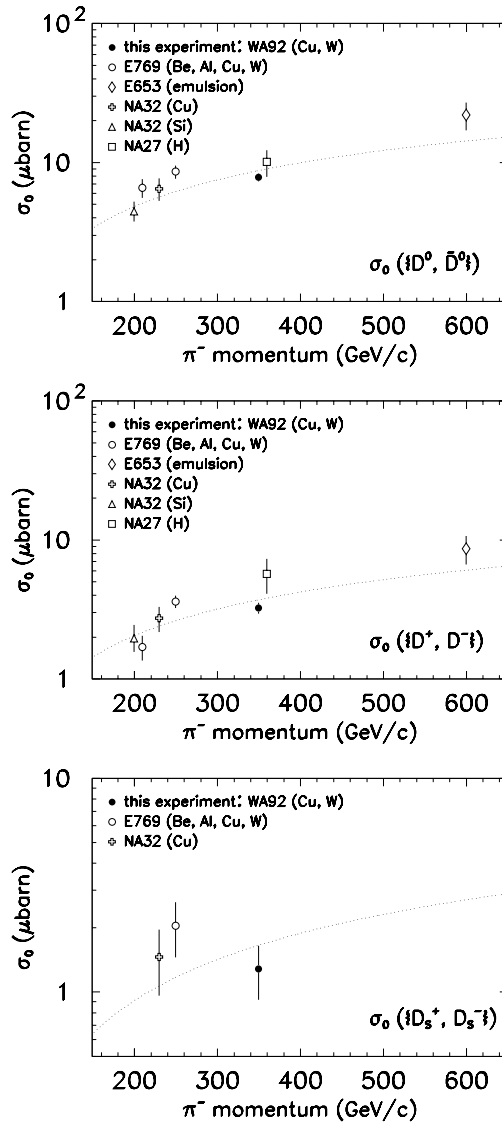


Figure 3: Cross sections for forward production of D mesons.

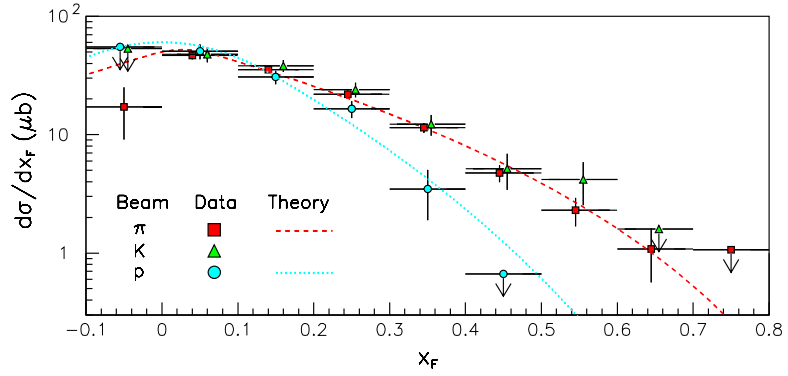


Figure 4: Differential Cross sections vs.  $x_F$  for D mesons from  $\pi$ -N collisions.

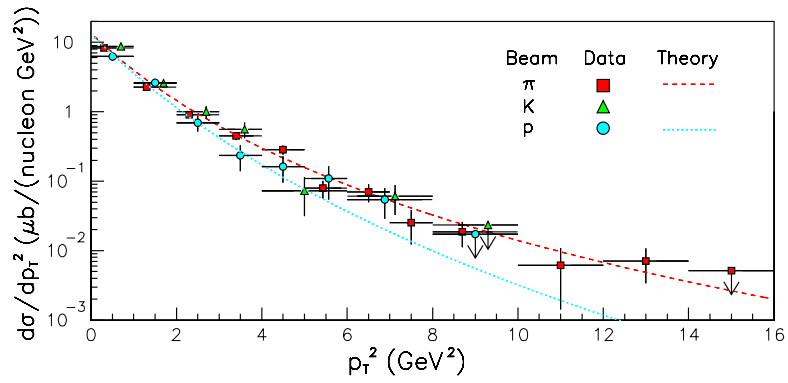


Figure 5: Differential Cross sections vs.  $p_T^2$  for D mesons from  $\pi$ -N collisions.

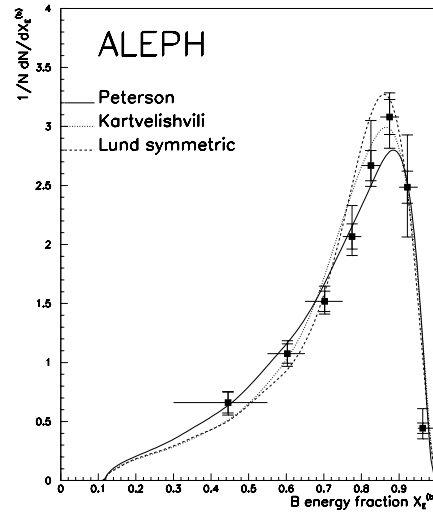


Figure 6: Fragmentation functions compared to ALEPH data.

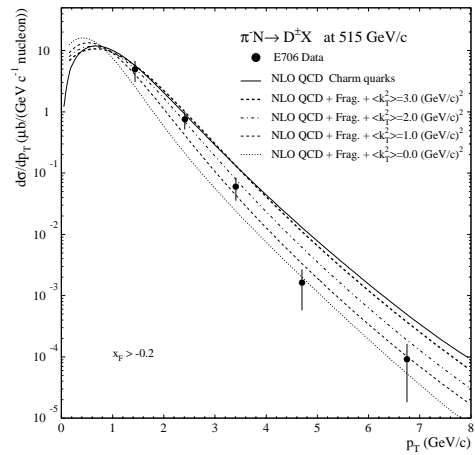


Figure 7: Differential cross sections vs.  $p_T^2$  from E706.

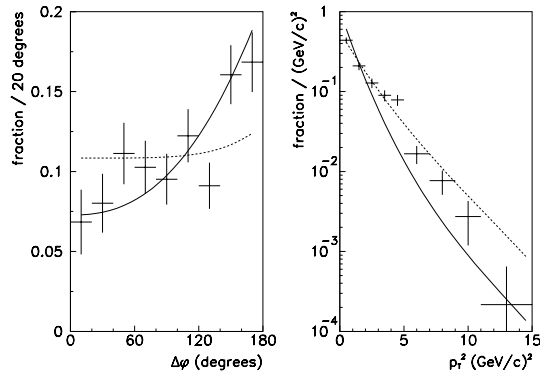


Figure 8: Azimuthal angle ( $\Delta\Phi$ ) between  $D$  and  $\bar{D}$  (left) and  $p_T^2$  of the  $D\bar{D}$  pair (right).

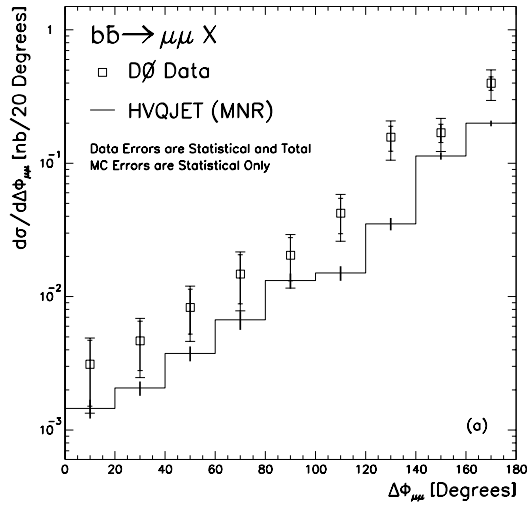


Figure 9: Azimuthal angle ( $\Delta\Phi$ ) between  $b$  and  $\bar{b}$  from  $D0$ .

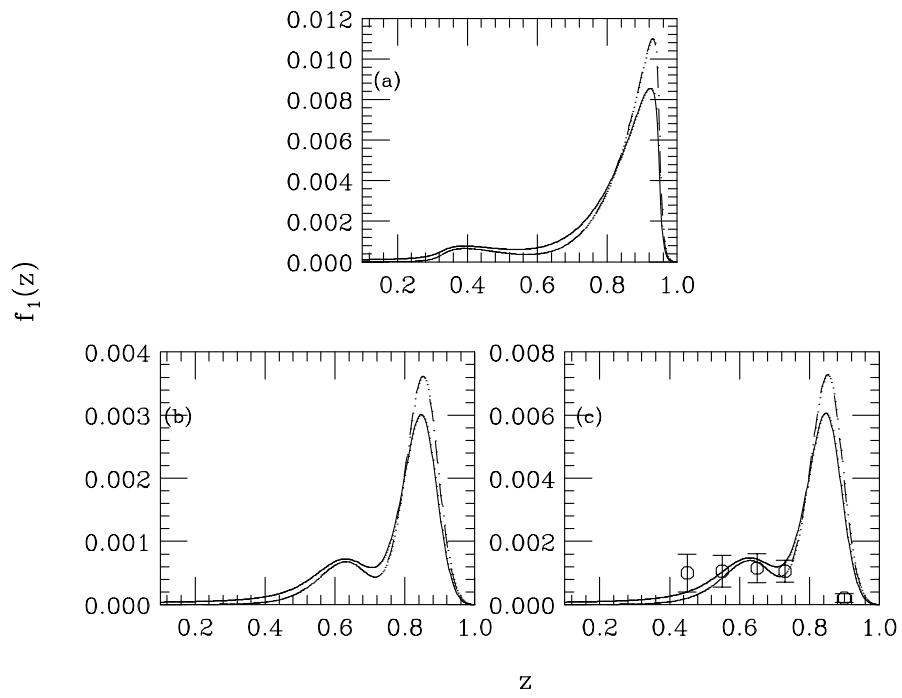


Figure 10: Baryon fragmentation functions for a)  $\Xi_c(1/2)$ , b)  $\Xi'_c(1/2)$ , and c)  $\Xi_c^*(3/2)$ .  $f_1(z)$  is the spin-averaged fragmentation function.

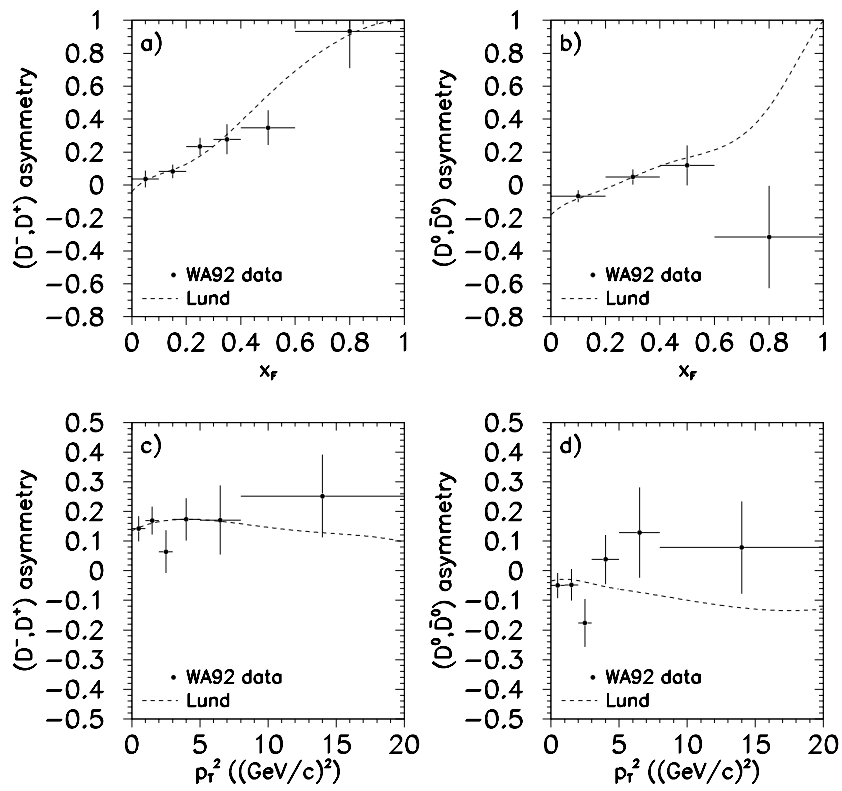


Figure 11: Asymmetry for forward production of D mesons from  $\pi$ -N collisions (WA92).

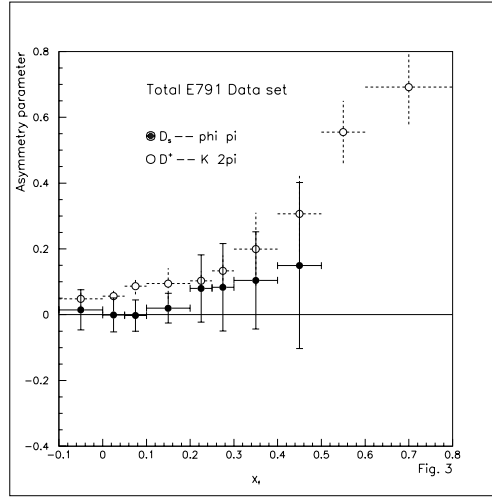


Figure 12: Asymmetry for  $D^+$  and  $D_s^+$  vs Feynman-x.

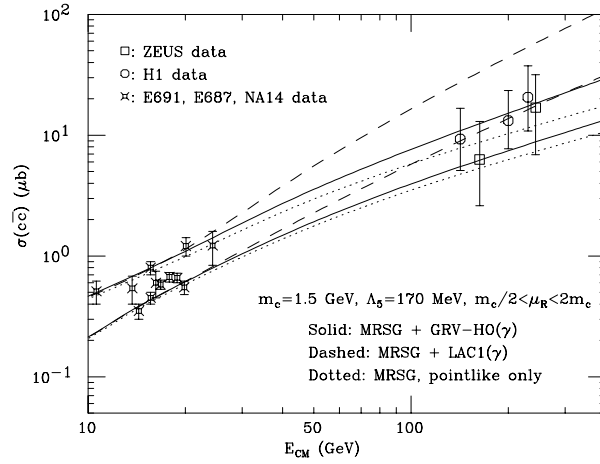


Figure 13: Cross sections for production of  $c\bar{c}$  from  $\gamma$ -p.

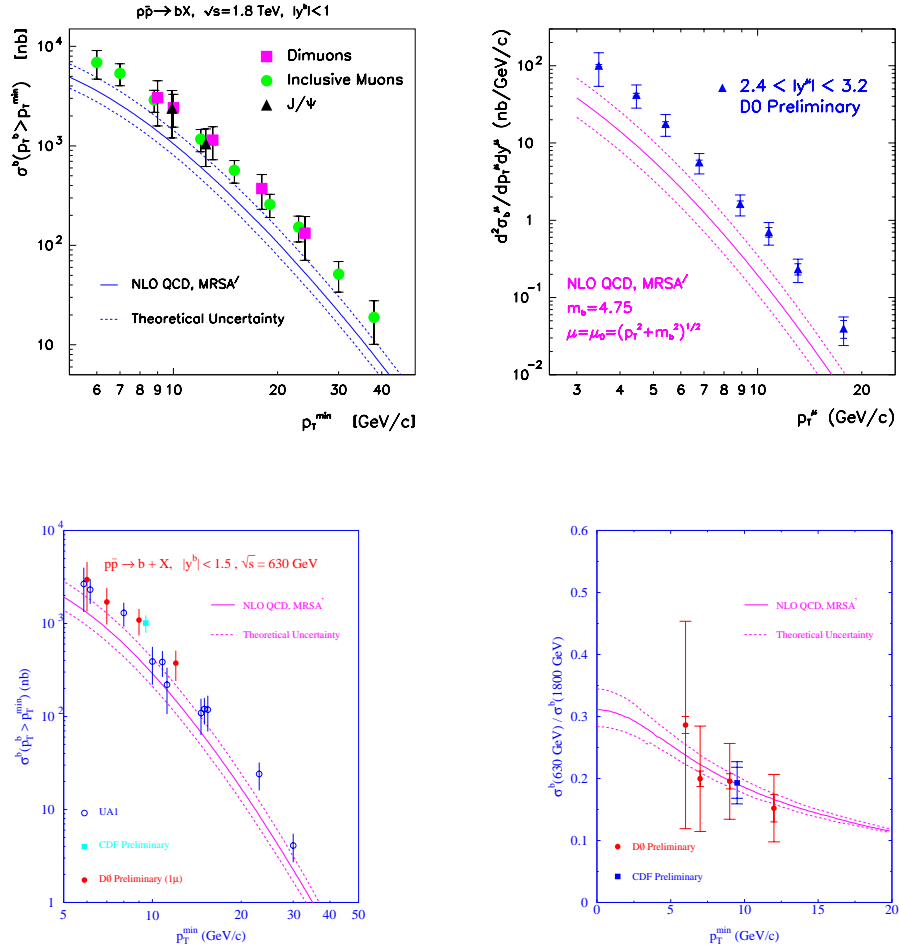


Figure 14: Inclusive b-quark cross sections at the Tevatron (upper left). Forward muon cross sections vs.  $p_t$  from D0 (upper right). Inclusive muon cross sections at 630 GeV from CDF and D0 (lower left). Ratio of muon cross sections at 1800 and 630 GeV (lower right).

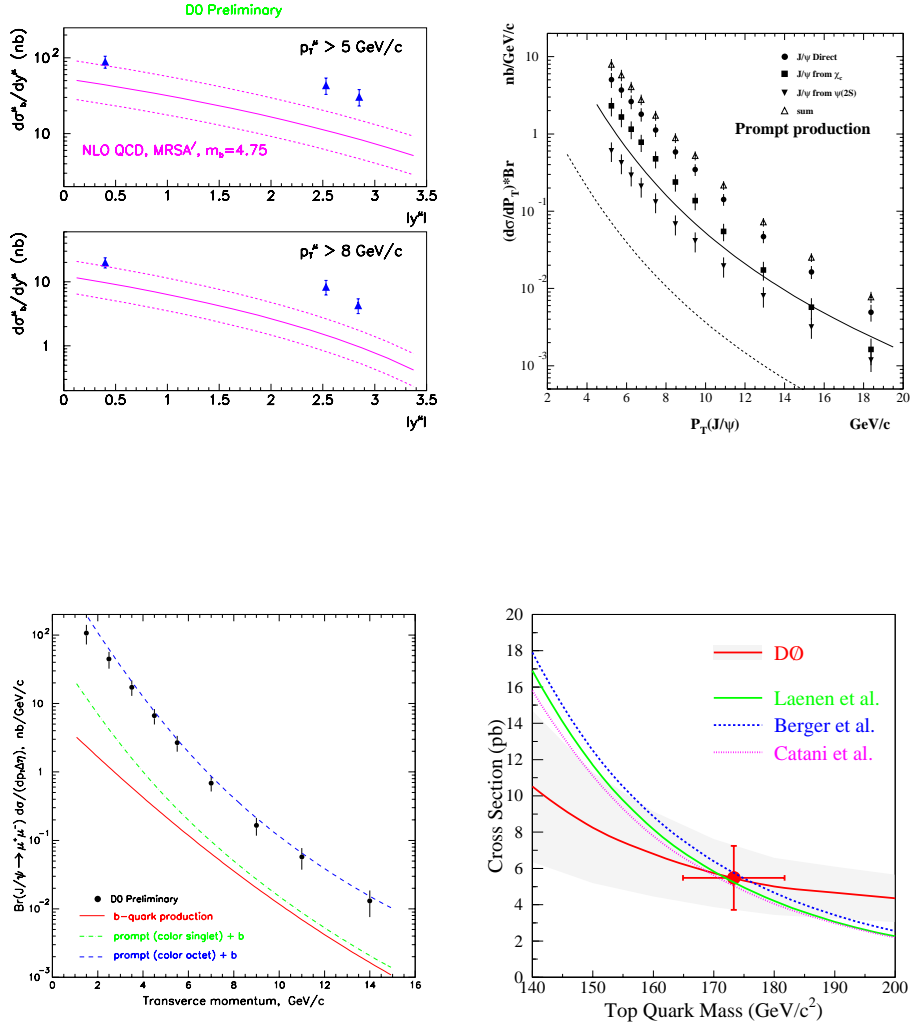


Figure 15: Forward muon cross sections vs. rapidity from D0 (upper left). Central  $J/\Psi$  cross sections vs. rapidity from CDF (upper right). Forward  $J/\Psi$  cross section vs.  $p_T$  from D0 (lower left). Inclusive top quark cross section measurement from D0 (lower right).